

Interpretable Transformation and Analysis of Timelines through Learning via Surprisability

Osnat Mokryn,¹ Teddy Lazebnik,² and Hagit Ben Shoshan¹

¹*Information Systems, University of Haifa, Israel*

²*Cancer Biology, Cancer Institute, University College London, London, UK*

(*Electronic mail: omokryn@is.haifa.ac.il)

(Dated: 7 March 2025)

The analysis of high-dimensional timeline data and the identification of outliers and anomalies is critical across diverse domains, including sensor readings, biological and medical data, historical records, and global statistics. However, conventional analysis techniques often struggle with challenges such as high dimensionality, complex distributions, and sparsity. These limitations hinder the ability to extract meaningful insights from complex temporal datasets, making it difficult to identify trending features, outliers, and anomalies effectively. Inspired by surprisability — a cognitive science concept describing how humans instinctively focus on unexpected deviations - we propose Learning via Surprisability (LvS), a novel approach for transforming high-dimensional timeline data. LvS quantifies and prioritizes anomalies in time-series data by formalizing deviations from expected behavior. LvS bridges cognitive theories of attention with computational methods, enabling the detection of anomalies and shifts in a way that preserves critical context, offering a new lens for interpreting complex datasets. We demonstrate the usefulness of LvS on three high-dimensional timeline use cases: a time series of sensor data, a global dataset of mortality causes over multiple years, and a textual corpus containing over two centuries of State of the Union Addresses by U.S. presidents. Our results show that the LvS transformation enables efficient and interpretable identification of outliers, anomalies, and the most variable features along the timeline.

I. INTRODUCTION

High-dimensional timeline data appears in numerous domains, from biomedical research to economic modeling and global monitoring¹⁻³. These high-dimensional datasets track multiple, often interdependent, features evolving over time, making their analysis both computationally and conceptually challenging^{4,5}. Detecting significant changes, identifying anomalies, and extracting meaningful insights often become intractable due to issues such as non-Gaussian distributions, sparsity, and high feature interdependence⁶⁻⁸. Traditional statistical and machine learning methods struggle to handle these complexities effectively, frequently requiring large labeled datasets or resorting to dimensionality reduction techniques that may obscure critical details^{9,10}. Transformation methods offer a powerful approach to address these challenges by converting raw data into more structured and interpretable forms¹¹.

Transformation methods have long been fundamental in mathematical analysis, signal processing, and data representation¹²⁻¹⁴. These techniques enable the conversion of complex problems into more interpretable forms (formally, computationally appealing representation), revealing underlying structures and facilitating efficient computations. Classical transformations, such as the Taylor series¹⁵ and Fourier transform¹⁶, allow function approximation and signal decomposition, making them useful for applications like noise reduction and image processing^{17,18}. However, these methods struggle with high-dimensional and nonlinear data, limiting their effectiveness in modern analytical tasks.

To address these limitations, more recent transformation methods provide structured representations for high-dimensional time-series data. Feature-based transformations¹⁹ extract key numerical descriptors, improving efficiency in tasks like anomaly detection and forecasting, but their reliance on predefined metrics may overlook critical patterns. Graph-based transformations^{20,21} leverage network structures to model dependencies and nonlinear relationships, yet their effectiveness depends on the chosen graph construction, which can introduce biases and distortions. Additionally, graph-based transformations can be computationally intensive, particularly for large-scale or real-time applications. While both approaches improve the representation of high-dimensional distributions, they also introduce abstraction layers that may obscure direct relationships and interpretability.

A fundamental challenge in transformation methods is balancing interpretability with computational efficiency. Existing transformation methods define a Pareto front between their performance and explainability^{22,23}. Classical techniques offer full analytical transparency but are often impractical for real-world data, while deep learning-based methods handle complexity but function as black boxes. Mokryn and Ben-Shoshan²⁴ attempted to push this Pareto front with LPA, an information-theoretic transformation that provided a structured yet efficient transformation of data that proved efficient in authorship attribution in social media and impersonation detection. The method was also applied to immunology data in the body²⁵. However, LPA and the other transformers are limited in their ability to capture time-series data.

Building on these advancements, we propose Learning via Surprisability (LvS), a transformation designed to highlight unexpected deviations in high-dimensional timeline data. By quantifying surprisal, LvS provides a structured and interpretable transformation that enables effective anomaly detection without requiring predefined labels or heuristics. Unlike existing methods

that either oversimplify data or obscure critical deviations, LvS maintains computational efficiency while offering a transparent, human-aligned representation of unexpected events.

The LvS transformation constructs an expected distribution over the entire timeline and represents each time bin by its most surprising features—those that deviate the most from this expected distribution. Intuitively, these are the features whose removal would most reduce the Jensen-Shannon (JS) divergence²⁶ between the time bin and the expected timeline distribution, thereby minimizing the Kullback-Leibler (KL) divergence²⁷. Thus, the retained features are those that contribute most to distinguishing each time bin from the overall timeline.

Three novel observations support the LvS transformation: (i) Unknown Known Features where popular timeline features that are missing or under-represented in a time bin are surprising and should be included in the time bin representation. These are the Unknown Known features; (ii) Per-Feature Divergence where Both KL and JS Divergence are the sum of a per-feature divergence; and (iii) Feature Surprisability where the features contributing most to the KL, and hence the JS divergence between a timeline representation (the expected) and a time bin, are the most surprising.

The proposed transformation aligns with the concept of surprisability, which quantifies the degree to which an event deviates from expected norms. Features that exhibit high surprisal are precisely those that cause the greatest divergence from the expected distribution. We hypothesize that this surprisability makes them the most informative in characterizing each time bin. By focusing on these features, LvS highlights the most unexpected yet significant variations in the data, offering an interpretable transformation that is both statistically grounded and cognitively aligned with how humans detect anomalies²⁸.

Surprisability is fundamental in human comprehension and cognitive processes, where it is also tied with expectations. For example, in understanding a sentence, Surprisal Theory maintains that the processing difficulty is related to probabilistic expectations and is defined as the log of the inverse of the probability of the event. Given an observed new event, e.g., a new observed word in a string, the information value of the event is the reciprocal of its probability^{29–32}.

In here, we present LvS, and demonstrate its power in identifying interpretable anomalies, outliers, and the most variable features along the timeline over three datasets, consisting of real-world sensor data, world main causes of death over a period of 30 years, and historical records.

The rest of this paper is organized as follows. Section II provides an overview of transformation methods, and Anomaly detection methods. Section III formally outlines the proposed Learning via Surprisability method. Section IV demonstrates LvS transformation over the two real-world time series datasets, and Section V demonstrates the LvS transformation over the timeline of textual data. Finally, section VI discusses the results in terms of possible applications and suggests future work.

II. RELATED WORK

In this section, we outline the applicative challenge LvS aims to tackle, as well as the computational methods in its base. Initially, we review the evolution of data transformation methods. Next, we review anomaly detections and their unique properties in high-dimensional and power-law distribution cases, followed by computational methods that use the distance between distributions for decision-making and the latent personal analysis algorithm.

A. Data transformation methods

The study of mathematical transformations is rooted in the fundamental need to represent data in a way that is beneficial for other tasks, such as anomaly detection³³, clustering³⁴, data compression³⁵, and others³⁶. As such, the transformation processes in mathematics and data science have evolved significantly, transitioning from classical methods such as Taylor series and Fourier transforms to contemporary data-driven techniques like Principal Component Analysis (PCA)³⁷ and autoencoders³⁸.

Initially, analytical transformations aimed to find an analytical representation of complex functions through a combination of simple-to-compute (and analyze) functions. For example, the Taylor series expansion, a foundational concept in calculus, allows functions to be approximated as infinite sums of their derivatives at a single point. This method is particularly powerful in solving differential equations, as demonstrated by the differential transform method (DTM), which reformulates differential equations into algebraic forms, enabling easier computation of solutions³⁹. The DTM has been successfully applied to various nonlinear differential equations, showcasing its versatility and efficiency in generating series solutions⁴⁰. Furthermore, the extension of the DTM to fractional calculus highlights its adaptability to more complex mathematical frameworks⁴¹. However, Taylor series expansion's reliance on smoothness and infinite series expansion limits its applicability to non-continuous or non-differentiable functions.

Thus, later, Joseph Fourier proposed the Fourier transform, which provides a different perspective by decomposing functions into their constituent sinusoidal components. By transforming a function from the time domain to the frequency domain, the Fourier transform provides a powerful framework for analyzing periodic signals, filtering noise, and solving differential equations^{42,43}. The Fourier transform's ability to convert convolution operations into multiplication simplifies many problems in engineering and physics, making it a cornerstone of modern analytical techniques⁴⁴. To this end, other methods, such as the

Laplace transform and the wavelet transform, further enhanced the ability to process signals with localized frequency content and transient behaviors^{45,46}.

While powerful, these classical transformations have limitations in handling complex, high-dimensional, and nonlinear data, which often fail to capture the intricate structures in real-world datasets, as these rely on predefined mathematical formulations⁴⁷⁻⁴⁹. This gives rise to machine learning (ML) and data-driven approaches to transformations that learn directly from data⁵⁰. The Principal Component Analysis (PCA), for instance, serves as a statistical transformation that reduces dimensionality by identifying the principal directions of variance in a dataset. Unlike Fourier analysis, which assumes an underlying sinusoidal basis, PCA finds an optimal basis that maximizes variance, making it effective in feature extraction and noise reduction. However, PCA traditionally assumes a linear basis (while one can also use any other functional analytical basis) which is not necessarily true. Going beyond linear transformations, autoencoders leverage neural networks⁵¹ to learn complex, non-linear transformations of data⁵². Through an encoder-decoder structure⁵³, autoencoders map high-dimensional data into lower-dimensional latent representations free from assumptions. Variants like variational autoencoders (VAEs) and transformer-based architectures further push the boundaries of learned transformations, allowing for probabilistic modeling and improved feature representations⁵⁴. This approach is particularly advantageous in scenarios with high-dimensional data, where traditional methods may falter due to the curse of dimensionality.

The evolution from classical transformations to data-driven techniques reflects a broader trend in mathematics and data science, where the focus has shifted toward methods that can handle the complexities of modern data sets⁵⁵. Recent years have introduced two additional transformation approaches for time series, feature-based and graph network transformations^{19,20}.

Feature-based time-series transformation involves extracting numerical descriptors that summarize key properties of temporal data, enabling tasks such as classification, clustering, and forecasting. Autocorrelation-based features capture dependencies between different time points by measuring how past values influence future ones. Entropy-based features measure the complexity or unpredictability of a time series. Other features characterize linear and non-linear dynamics or try to identify the generative structure of the data¹⁹.

The transformation of time series into graph networks leverages complex network theory and graph properties, thus enabling the analysis of the structural and topological features of the data^{20,21}. This transformation enables the study and detection of nonlinearity, chaos, extreme events, fluctuations, and temporal dynamics, including points of change^{21,56-59}. Recently, time series of human interactions have been transformed into temporal complex networks to investigate the dynamics of human interplay and viral propagation, as well as the spread of pathogens in populations⁶⁰⁻⁶².

In here, we suggest a timeline transformation algorithm that enables interpretable anomaly and outlier detection. The method borrows some of its concepts from Latent Personal Analysis, explained next.

B. Anomaly and outlier detection

In domains like financial markets, network traffic, and sensor data, detecting anomalies is vital for monitoring, security, and accurate analysis⁶. In these real-world domains, however, the data is high dimensional, making the task quite challenging. Generally, anomaly detection (AD) serves as a vital keystone in machine learning, data analysis, and statistics, permeating nearly every field that grapples with quantitative data. At its core, AD involves uncovering patterns, observations, or events that stray far from the expected rhythm of normalcy⁶³—these rare deviations, often dubbed anomalies or outliers, frequently signal critical yet uncommon occurrences^{64,65}, which more often than not considered interesting due to their unusual (or somewhat surprising) nature. From the early diagnosis of mechanical failures⁶³ to unmasking financial fraud⁶⁶, fortifying cybersecurity⁶⁷, refining decision-making⁶⁸, and enabling real-time clinical alerts⁶⁹, the impact of AD resonates across domains, illuminating the unseen and the unexpected. In a data-driven context, AD is often seen as a distinct branch of machine learning, formally represented as a binary classification problem where one is tasked to sort data into normal and anomalous samples^{70,71}. Yet, the elusive nature of anomalies renders traditional classification models ill-equipped for the task, as they are tuned to the majority and falter in capturing rare (surprising) instances. This limitation has sparked the creation of specialized algorithms, meticulously designed to unveil the hidden and the unexpected⁷², such as Gaussian mixture models³³, Mahalanobis distance⁷³, hypothesis testing⁷⁴, and convex hull-based AD⁷⁵. These approaches operate under the assumption that the data follows a defined statistical distribution in the same dimension of the samples, flagging any points that markedly deviate from this expected pattern as anomalies. More recent methods use advances in machine learning methods⁷⁶ which fall into three broad categories: supervised, semi-supervised, and unsupervised approaches. Supervised techniques, such as neural networks and support vector machines, rely on labeled datasets containing both normal and anomalous instances. However, in practical applications, obtaining such labels proves challenging due to the high cost and complexity of data annotation⁷⁷. Semi-supervised methods, including One-Class SVM⁷⁸, One-Class deep neural networks⁷⁹, autoencoders⁸⁰, and local outlier factor⁸¹, circumvent this issue by training exclusively on normal data, identifying anomalies as deviations from learned patterns⁸². Unsupervised methods involve optimizing a gain function⁸³ or modeling an underlying distribution⁷⁵. These methods are usually the easiest to apply in real-world scenarios as these do not require labeled data or domain expertise. While these methods excel at capturing statistical or learned deviations, they often reduce dimensions and simplify the data, making the results uninterpretable, and missing rare yet significant

anomalies. Timeline Analysis via Surprisability addresses this gap by introducing an additional temporal dimension, allowing the model to uncover unexpected features and detect anomalies that traditional methods might overlook.

Practically, long tail and power-law distributions are prevalent in nature and empirical data⁸⁴⁻⁸⁷, particularly in high-dimensional domains such as biology⁸⁸ and language⁸⁹. For instance, B-cell repertoires and single-cell transcriptomic data often follow long-tail distributions, where a few dominant features (e.g., highly expressed genes or dominant B-cell clones) account for most of the variability, while the majority occur infrequently^{25,90}. Similarly, in language, word frequencies—treated as categorical data—follow Zipf’s law, a classic example of a power-law distribution⁹¹. Analyzing empirical high-dimensional data is inherently challenging due to its exploratory nature and the lack of labeled data, necessitating unsupervised methods⁶³. The complexity of high-dimensional spaces often leads to difficulties in identifying anomalies due to the^{92,93}, where the distance metrics used in traditional anomaly detection methods become less effective as dimensionality increases^{94,95}. This phenomenon is exacerbated in multivariate contexts, where the interaction between multiple dimensions can obscure the identification of outliers⁹⁶.

Distributions in the power-law family are commonly used for anomaly detection as a portion of the samples are common while others are extremely rare⁹⁷. This kind of analysis is relatively easy for low-dimensional data, but as the number of features (and therefore dimensions) grow larger, the analysis becomes both conceptually and computationally more challenging^{6,98}.

Various methodologies have been proposed to address these challenges^{63,99,100}. For example,¹⁰¹ introduced a hybrid anomaly detection method that leverages autoencoders to transform high-dimensional classification datasets into formats suitable for anomaly detection. This approach highlights the importance of dimensionality reduction techniques, which are essential for enhancing the performance of anomaly detection algorithms in high-dimensional settings¹⁰². Dimensionality reduction not only helps in mitigating computational costs but also improves the interpretability of the data, allowing for more effective anomaly identification¹⁰³.

Moreover, the application of advanced machine learning techniques, such as Generative Adversarial Networks and deep learning architectures, has shown promise in improving anomaly detection accuracy in high-dimensional datasets^{104,105}. These methods are particularly beneficial in scenarios where traditional statistical methods falter, as they can learn complex patterns and relationships within the data that are indicative of normal behavior, thereby facilitating the identification of anomalies¹⁰⁶.

Currently, there are widely adopted unsupervised anomaly and outlier detection methods considered state-of-the-art. Among them are the following. First, the Isolation Forest⁸¹ algorithm isolates individual data points through recursive partitioning of the data space, identifying outliers based on the speed (i.e., number of partitions) at which they can be separated. It constructs an ensemble of isolation trees, where data points that are isolated with shorter average path lengths are flagged as anomalies. This method relies solely on the ordinal ranking of each variable, disregarding distances and inter-variable relationships. Thus, its effectiveness may be diminished in situations where these factors are critical, like in high-dimensional spaces. Second, *Single-Class SVM*^{79,107} detects anomalies by learning a boundary around normal data. Trained on data from a single class, these methods assume points outside the learned boundary are anomalous. *Single-Class SVMs* construct a hyperplane that maximally separates normal data from the origin. Third, *Local Outlier Factor (LOF)*¹⁰⁸ measures the local density deviation of a data point relative to its neighbors, identifying outliers in areas of significantly lower density. This method detects abnormality without considering the global structure of the data and, therefore, will under-perform in cases where the context of the data can shed more light on its place in a distribution represented by a more computationally meaningful space.

C. Latent Personal Analysis

Measuring the distance between distributions is a key technique widely used in identifying changes over time, detecting anomalies, and identifying outliers^{63,109,110}. It is also used for classification and decision-making, as shown in¹¹¹, which established KLD and Jensen-Shannon Divergence as metrics for assessing document similarity.

Latent Personal Analysis (LPA) is a recently suggested method for characterizing and comparing high-dimensional distributions in a population, where the population is an *aggregation* of the entities within it²⁴. For example, when considering textual data, LPA can be used to characterize a book (population) and its chapters (entities within the population), when the tokens (words) are represented by their frequencies. LPA identifies the most "surprising" words in each chapter when the chapter’s frequency probability distribution is compared with the book’s one. These surprising elements are determined based on Shannon information¹¹², computed using the Kullback-Leibler Divergence (KLD)^{27,113}. KLD is used as it is a distance metric that takes into account small changes in the tail of the distribution.

Technically, LPA identifies the elements that contribute most to this information gain and uses them as the entity’s representation given that KLD measures the information gain from using an entity’s distribution (Q) to model the population distribution (P). Thus, LPA captures the entity’s most distanced (and therefore "surprising") elements relative to an expected population and assigns them a weight corresponding to their distance (surprisal), i.e., their contribution to the information gain.

Interestingly, an entity’s surprising elements can include population-prevalent elements that are underrepresented or missing in the entity. LPA incorporates such elements into the entity’s representation with a weight proportional to their surprisal but

with a negative sign. This reflects the understanding that “what is missing” can carry important information, echoing Freud’s insight that “the missing, not conveyed, is an integral part of the whole.”

Formal Description. Let $\{Q_i(x)\}, i \in N$, where N is the number of entities, represent a set of entities, each with a probability distribution $Q_i(x)$ over a possibility space of elements \mathcal{D} .

The population element-frequency distribution $P(x)$ is defined as the normalized aggregation of the entities’ distributions:

$$P(x) = \frac{\sum_{i=1}^N Q_i(x)}{\sum_{i=1}^N \sum_{x \in \mathcal{D}} Q_i(x)}$$

Here, $P(x)$ represents the probability of each element $x \in \mathcal{D}$ in the population.

To account for variability in vector lengths and the long tail of rare elements in $P(x)$, LPA modifies each entity’s distribution $Q_i(x)$ by extending its support. Missing elements are assigned a small constant value ε , as described in Bigi’s method¹¹⁴:

$$\forall i \in \{1, \dots, N\} : Q_i(x) \rightarrow \tilde{Q}_i(x) = \begin{cases} \beta_i Q_i(x) & \text{if } Q_i(x) > 0 \\ \varepsilon & \text{if } Q_i(x) = 0 \end{cases}$$

where β_i ensures normalization:

$$\sum_{x \in \mathcal{D}} \tilde{Q}_i(x) = 1 \quad \Rightarrow \quad \beta_i = 1 - \varepsilon \cdot \#\ker(Q_i)$$

Here, $\#\ker(Q_i)$ denotes the number of elements $x' \in \mathcal{D}$ where $Q_i(x') = 0$.

LPA uses the symmetrized KLD to compute the divergence between an entity $Q_i(x)$ and the population $P(x)$:

$$\tilde{D}_{KL}(P\|Q_i) = \frac{1}{2} (D_{KL}(P\|Q_i) + D_{KL}(Q_i\|P))$$

where

$$D_{KL}(P\|Q_i) = \sum_{x \in \mathcal{D}} P(x) \log_2 \left(\frac{P(x)}{Q_i(x)} \right)$$

Surprisability Calculation. The surprisal of an element $x \in \mathcal{D}$ is defined as its per-element contribution to the symmetrized KLD:

$$S(x) = (P(x) - Q_i(x)) \cdot \log_2 \left(\frac{P(x)}{Q_i(x)} \right)$$

Elements with the highest surprisal values form the entity’s LPA representation. For missing or underrepresented elements, $S(x)$ is computed with a negative sign.

Each entity’s LPA representation consists of the top surprising elements: The k elements with the highest surprisal values, where k is determined as discussed in²⁴. Additionally, an entity has a divergence attribute, corresponding to the total divergence between the entity $Q_i(x)$ and the population $P(x)$: $D(Q_i, P) = \sum_{x \in \mathcal{D}} S(x)$. Taken jointly, LPA provides both quantitative and qualitative insights into entities in a population. By incorporating missing elements, LPA captures additional information, enhancing its utility for understanding high-dimensional distributions^{24,25}.

Notably, due to the ε -padding process for missing elements, LPA often exaggerates the significance of rare or new events, such as newly used words or misspellings on platforms like Twitter, even if their probabilities are only slightly above the designated ε value. Additionally, LPA’s aggregation of entities to a population is not suitable for timelines.

III. TIMELINE TRANSFORMATION USING LEARNING VIA SURPRISABILITY

A. Motivation

“*He who knows, and knows not that he knows, is asleep; wake him*”, — a quote from the Persian philosopher Ibn Yami — highlights the significance of “unknown knowns”, referring to knowledge that exists but remains unrecognized. The concept of unknown knowns is pivotal across fields such as decision-making, risk assessment, psychology and cognition, and plays a critical role in explaining biases.

This work builds on the observation that a transformation of a collection of time bins or entities along a time axis can be used to infer the surprising elements in each time bins and can efficiently represent each entity through elements that most differentiate it from a time axis transformation. Inspired by human cognitive processing of surprisal, we hypothesize that the most surprising elements relative to a population capture an entity’s essence, revealing its “unknown knowns”—common elements underrepresented or absent in the entity. This contrast enables anomaly and change detection by highlighting deviations and shifts in expected patterns.

B. LvS transformation algorithm

Let \mathcal{T} denote a time axis (or timeline). We assume here that the timeline period is known and that N is the total number of bins in the timeline \mathcal{T} ¹⁵. We define $T_i, i \in [1..N]$, as the high-dimensional probability distribution of elements at time bin i . Each T_i distribution comprises a set of elements $E_i \subseteq \Omega$, where Ω is the set of all elements that appear in any of the bins in \mathcal{T} . In our case, we use the terms element and feature interchangeably.

We characterize a time axis \mathcal{T} that consists of N high dimensional probability distributions using a timeline center representation for the timeline, and a surprisability profile for each of the time bins in the timeline, as follows.

1. Creating a Timeline Center Representation

Central to the method is the creation of an *Information Science Center* of a timeline as its center representation. The Timeline Center Representation (*TCR*) is a distribution that consists of the mean value for each element $e \in \Omega$, calculated across all time bins. An element e can be in an arbitrary k number of time bins, $1 \leq k \leq N$, where N is the total number of time bins in \mathcal{T} . We determine the *TCR* by calculating the average value for each element across all time bins in the timeline. If an element is missing in a specific time bin distribution T_i , it is calculated as zero, as if this time bin added zero to the mean.

The Timeline Center Representation (*TCR*) is then calculated as follows:

$$TCR(j) = \frac{1}{N} \sum_{i=1}^N T_i(j) \cdot \mathbb{I}(\text{element } j \text{ exists in } T_i) \quad (1)$$

$$TCR = \{TCR(j), j \in \Omega\} \quad (2)$$

Sorting the *TCR* in decreasing order of mean relative frequencies will yield a ranked list of the elements, according to their *relative prominence* in the timeline.

2. Creating a time bin Surprisability Profile:

For a given time bin distribution T_i within a timeline, the Surprisability Profile (*SP*) represents the subset of elements $e \in \Omega$ that are most surprising given the expectation as represented by *TCR*. We determine these elements by calculating the Jensen-Shannon divergence (*JSD*) between the *TCR* and each of the time bin distributions T_i is defined, and then determining the most surprising elements.

$$JSD(TCR, T_i) = \frac{1}{2} KLD(TCR, M_i) + \frac{1}{2} KLD(T_i, M_i) \quad (3)$$

where

$$M_i = \frac{1}{2}(TCR + T_i) \quad (4)$$

and *KLD* denotes the asymmetric Kullback-Leibler divergence.

We then identify the time bin's surprisability profile as follows. For each time bin i , the *JSD* calculated between the center and the time bin, created a per-element divergence between the value of the element in the time bin (zero if missing) and their mean value in the *TCR*, which is a non-zero value. Consequently, the process generates SP_i , a local vector representation of the time bin's distribution, defined as:

$$\forall j \in \Omega, \quad SP_i(j) = \left(\frac{1}{2} TCR(j) \log_2 \left(\frac{M_i(j)}{TCR(j)} \right) + \frac{1}{2} T_i(j) \log_2 \left(\frac{M_i(j)}{T_i(j)} \right) \right) \cdot \mathbb{I}(\text{element } j \text{ exists in } T_i) \quad (5)$$

Let D_i denote the distance of time Bin T_i from the *TCR*, given by:

$$D_i = \sum_{j=1}^{\Omega} |SP_i(j)| \cdot \mathbb{I}(\text{element } j \text{ exists in } T_i) \quad (6)$$

We then set the weight in SP_i , which is now the difference from the mean weight of that element in the timeline, to indicate whether it is locally overused or underused compared with its mean value over the period, as follows:

$$\forall j \in \Omega, \quad SP_i(j) = \mathbb{I}(\text{element } j \text{ exists in } T_i) \cdot \begin{cases} SP_i(j) & \text{if } M_i(j) \geq TCR(j) \\ -SP_i(j) & \text{if } M_i(j) < TCR(j) \end{cases} \quad (7)$$

The next step is to determine the subset of elements in SP_i for which the calculated value is sufficiently surprising. Only elements that exceed a predefined surprisability threshold θ will be retained to define SP . Formally, this subset is given by:

$$SP_i^\theta = \{j \in SP_i \mid |SP_i(j)| > \theta\} \quad (8)$$

where θ denotes the surprisability threshold. The elements in SP_i^θ represent those considered significantly surprising within the time bin i .

LvS transformation identifies each time bin T_i by two representations. The first is its JS divergence, and the second is its Surprisability Profile, as follows.

LvS distance: D_i is a measure of how different is T_i from the dataset when the TCR is expected. It is calculated as the sum of the absolute values of the JSD differences of T_i 's elements from their corresponding elements in the TCR 's, where timeline prominent elements that are missing from T_i contribute to this distance. D_i is defined in Eq 6.

LvS SP: SP_i^θ is a low dimensional interpretable presentation of T_i that includes the most surprising elements in T_i when TCR is expected. The threshold-based surprisability profile, SP_i^θ , is defined in Eq 8.

IV. TIMELINE ANALYSIS WITH LVS: TIMESERIES

LvS's approach of finding the uniqueness of each time bin compared with the timeline while accounting for latent elements along the timeline enables timeline and timeseries analysis, as is demonstrated in the following.

1. Analyzing SWaT: Multimodal Time Series Anomaly (Attack) Prediction

In order to empirically evaluate LvS's performance with respect to the current state-of-the-art results, we adopted the popular *SWaT dataset*^{116–118}, a real-world data from the Secure Water Treatment plant testbed, a testbed built at the Singapore University of Technology and Design¹¹⁹, and publicly available (https://itrust.sutd.edu.sg/itrust-labs_datasets/dataset_info/). The SWaT dataset describes a computational system's state over time with 450 thousand records and 51 features for each record. Out of these, around 12% of the records are manually tagged as cyber security attack attempts.

The SWaT dataset consists of sensor and actuator data collected from a fully operational six-stage water treatment process. It contains two main types of data: *Normal Operation Data*: collected over 7 days, where the system was operating under standard conditions without cyber or physical attacks. *Attack Data*: Collected over 4 days, during which a total of 41 carefully designed cyber-physical attack scenarios were executed. These attacks include sensor spoofing, actuator manipulation, and communication disruptions, targeting different stages of the water treatment process. The dataset consists of time-series records where each row represents a timestamped instance of system behavior, including sensor readings (e.g., flow rates, water levels, pressures, and conductivity), actuator states (e.g., pump status, valve positions), and labels denoting whether this is normal operation or an attack.

First, we predict the anomalies using the **LvS Distance** representation and compare the performance to state of the art unsupervised algorithms. Our hypothesis is that if the majority of the time bins register the system state during normal operation, the JS Divergence of time bins registering the system state when under attack would be larger, and hence their LvS Distance would be bigger.

We use the LvS transformation over the SWaT data, and train the Isolation Forest, LOF, and One-class SVM models on attack detection. In order to avoid differences in decision threshold optimization, the optimal recall-precision threshold is used for all algorithms. Table I shows the results of this analysis in terms of the model's area under the receiver operating characteristic curve (AUC), recall (sensitivity), precision, F_1 score, and accuracy. Notably, LvS obtains the highest AUC value (82.3%) followed by a large margin by Isolation Forest with 54.5%. For precision, the Isolation Forest obtains the highest precision (97.5%) while achieving a recall of 8.0% while one-class SVM received a precision of 91.3% and recall of 76.0% which also results in the highest F1 score of 83.0% followed by LvS. Taken jointly, while the one-class SVM is able to differentiate between the anomaly

Metric	LvS	Isolation Forest	LOF	One-Class SVM
AUC	82.3%	54.5%	50.3%	9.1%
Precision	69.9%	97.5%	22.9%	91.30%
Recall	69.9%	8.0%	3.4%	76.0%
F1 Score	69.9%	14.8%	5.8%	83.0%
Accuracy	92.7%	88.8%	93.4%	96.21%

TABLE I. Performance comparison of different anomaly detection methods, the best value of each metric is highlighted in bold font.

and regular records the best, its decision threshold, as indicated by its low AUC score (9.1%) is hard to find and therefore deeming the results unstable. Unlike, while second in most metrics, LvS shows consistent performance across all five metrics.

Moreover, as these results are obtained for the optimal decision threshold, they may not reflect the performance of LvS in applicative settings. As such, we conducted a sensitivity analysis around the optimal decision threshold, analyzing the performance of LvS for each case. Table II presents the results of this analysis, where a distance of ten percent from the optimal decision threshold results in a drop of two percent in both recall and precision. The change in the AUC and accuracy is even smaller, with less than a one percent decline.

Metric	-10%	-5%	0%	5%	10%
AUC	81.8%	82.4%	82.9%	83.3%	83.6%
F1 Score	67.9%	69.0%	69.9%	70.8%	71.3%
Precision	67.9%	69.0%	69.9%	70.8%	71.3%
Recall	67.9%	69.0%	69.9%	70.8%	71.3%
Accuracy	92.3%	92.5%	92.7%	92.9%	92.9%

TABLE II. Decision threshold sensitivity analysis for LvS on the SWAT dataset.

We continue here and evaluate the performance of our transformation in identifying anomalies using the **LvS SP** representation.

The hypothesis is that the SP of time bins during normal operation will resemble each other more than the SP of time bins during attacks. To prepare the LvS data for K-means clustering, a scaling procedure was applied to eliminate negative values. The preprocessing consisted of two steps: first, vector elements were multiplied by 10, and then a constant of 0.4 was added to ensure non-negativity. The scaled LvS vectors were then processed with PCA before clustering using K-means with 2, 3, and 5 clusters. The clustering performance was assessed by comparing the generated cluster assignments with the predefined 'Attack' labels. The clustering results confirm the effectiveness of the LvS SP representation in distinguishing normal operation from

TABLE III. Confusion Matrix and Performance Metrics

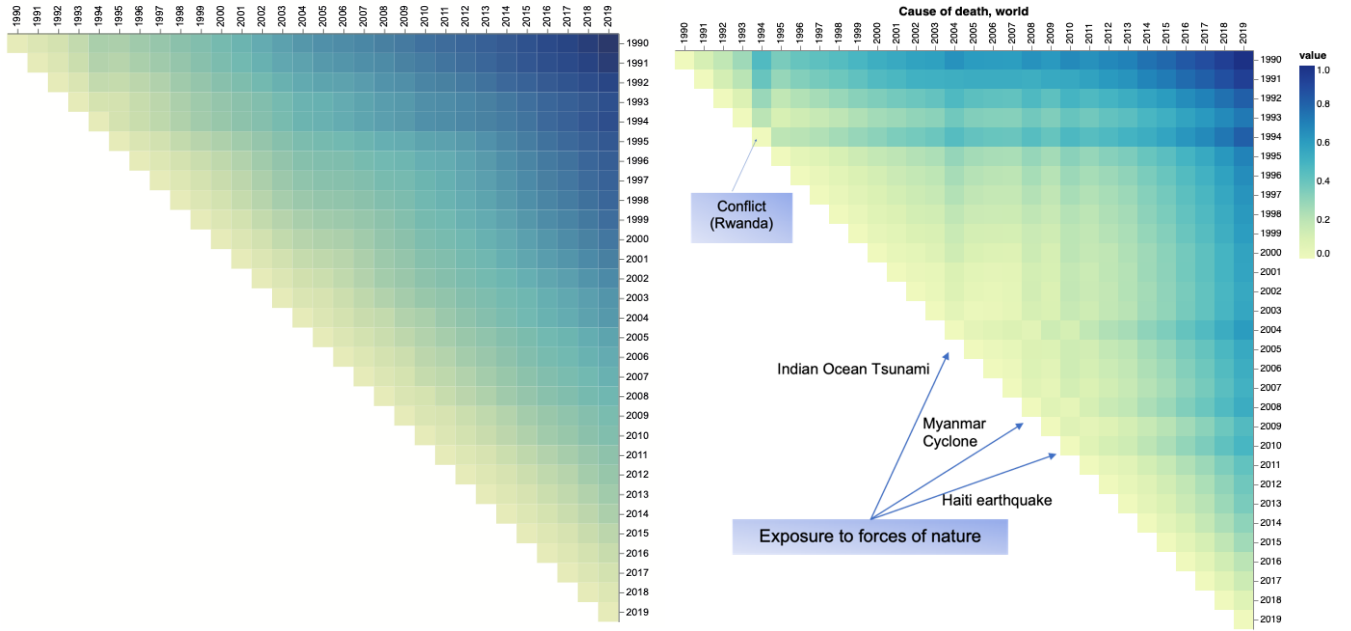
True Label	Cluster 0	Cluster 1	Total (Actual)
Normal Operation	395,187	111	395,298
Attack	22,661	31,960	54,621
Total (Predicted)	417,848	32071	

Metric	Cluster 0	Cluster 1
Precision	0.9458	0.9965
Recall	0.9997	0.5851
F1 Score	0.9720	0.7373
Overall F1 Score	0.8547	

attacks. Cluster 0 captures most normal instances with 0.9997 recall, while Cluster 1 identifies attacks with 0.9965 precision, though its lower recall (0.5851) indicates missed detections. The overall F1 score of 0.8547 reflects strong but imbalanced classification. Clustering with 3 and 5 clusters yielded poor performance and was therefore omitted.

2. Interpretable Outlier and Anomaly Detection

To demonstrate visually the power of LvS in interpretable outlier and anomaly detection, we use here a smaller dataset of 30 years of major causes of death (CoD) in the world^{120,121}. The dataset describes the main causes of death in the world in the period of 1990 to 2019. Deaths are attributed to an underlying cause, as opposed to deaths that happen due to risk factors, e.g.,



(a)Distance measure across all time bins' distributions in world mortality data (b)Distance measure across all time bins' SPs, identifying points of change in of 30 years, original data world mortality reasons

FIG. 1. Analysis of causes of death over 30 years: (a) A comparison of the original vectors representing causes of death over a 30-year period. Each square corresponds to the comparison of probability distribution vectors between two years, with lighter colors indicating greater similarity. The figure clearly shows that any two consecutive years exhibit a high degree of similarity in the underlying causes of death worldwide. (b) A comparison of the Surprisal Profile vectors created by LvS of the causes of death over a 30-year period. Each square corresponds to the comparison of the SP probability distribution vectors between two years, with lighter colors indicating greater similarity. Notable anomalies are clear in the years 1994, 2004, 2008, and 2010. The values within the SP vectors enable interpretation of the most surprising elements causing the anomaly in these years. Values were normalized for easier reading.

smoking¹²⁰. Ending in 2019, this dataset does not include the Covid-19 years. The CoD dataset contains, for each of the years 1990 to 2019, the number of deaths at each year worldwide from the top 30 death causes.

To prepare the dataset for the LvS transformation, we create yearly probability distributions (time bins) of the causes of death, as explained here. We obtained the world population for each year, calculated the percentage of deaths for each of the 30 causes relative to the total population, and then constructed a probability distribution vector representing the percentage of worldwide deaths attributed to these main causes for each year. We start with a visually interpretable anomaly detection, and continue with a numerical analysis.

Here, we use the **LvS SP** feature in the following way. We construct two matrices, A , and ASP . Each entry A_{ij} (ASP_{ij}) represents the L_1 distance (Manhattan distance) between the probability distribution vectors (SP vectors) as follows

$$A_{ij} = \sum_{k \in [1..30]} |V_i(k) - V_j(k)|, \forall i, j \in [1990 \dots 2019], ASP_{ij} = \sum_{k \in [1..30]} |SP_i^\theta(k) - SP_j^\theta(k)|, \forall i, j \in [1990 \dots 2019].$$

Figure 1 presents a visual side-by-side comparison of A and ASP , that is, the cross-comparison results between the yearly probability distribution vectors (Figure 1 (a)) and the yearly SPs (Figure 1 (b)). Each square represents a comparison between two years, as indicated by the corresponding row and column, with lighter colors denoting greater similarity. The distance matrices were normalized before applying the coloring.

Figure 1 (a) clearly illustrates that consecutive years exhibit a high degree of similarity in the underlying causes of death worldwide. There is a high correlation between subsequent time bins, and the divergence of change is subtle and incremental. Death rates associated with diseases, illnesses, and other health factors, which account to the majority of world-wide deaths, generally evolve gradually over time. While they may fluctuate slightly from year to year as part of broader trends, significant shifts are uncommon, disregarding natural disasters and terrorism-related deaths¹²¹.

Indeed, when comparing the SP vectors across the years, as shown in Figure 1 (b), we obtain a visually interpretable method for outlier detection, where significant change points become evident. This allows for the identification of specific moments in time when natural disasters and terrorism-related deaths peak. The SP also indicates the most surprising feature, as depicted in Figure 1 (b). These findings are the same as the in-depth analysis conducted by Max Roser *et al.*¹²¹. A change was evident in

1994, and the corresponding most surprising element in the SP is *conflict*. It is attributed to the genocide in Rwanda in 1994, that “stands out for its very high death-toll”¹²¹. The years 2004, 2008, and 2010 all are anomalous. In these years, the most surprising feature is *exposure to forces of nature*, corresponding to the 2004 Indian Ocean earthquake and tsunami; Cyclone Nargis which struck Myanmar in 2008; and the 2010 Port-au-Prince earthquake in Haiti¹²¹.

In summary, LvS transformation enables interpretable anomaly detection.

3. A Measure of Dynamics: Identifying the Most Variable Features

We define highly variable features as those that exhibit significant fluctuations across the timeline, reflecting substantial temporal changes in the high-dimensional distributions. A key measure of timeline dynamics, where each time bin represents a high-dimensional distribution, is the extent to which individual features vary over time. Unlike traditional approaches that primarily capture trends, our method, LvS, uniquely identifies time bins in which certain features are missing or underutilized. This provides a more comprehensive view of feature dynamics, ensuring that critical variations are not overlooked. Additionally, LvS effectively pinpoints the features that undergo the most significant changes along the timeline, offering deeper insights into temporal variability. To identify the terms that were the most highly variable across the timeline, we looked for those that

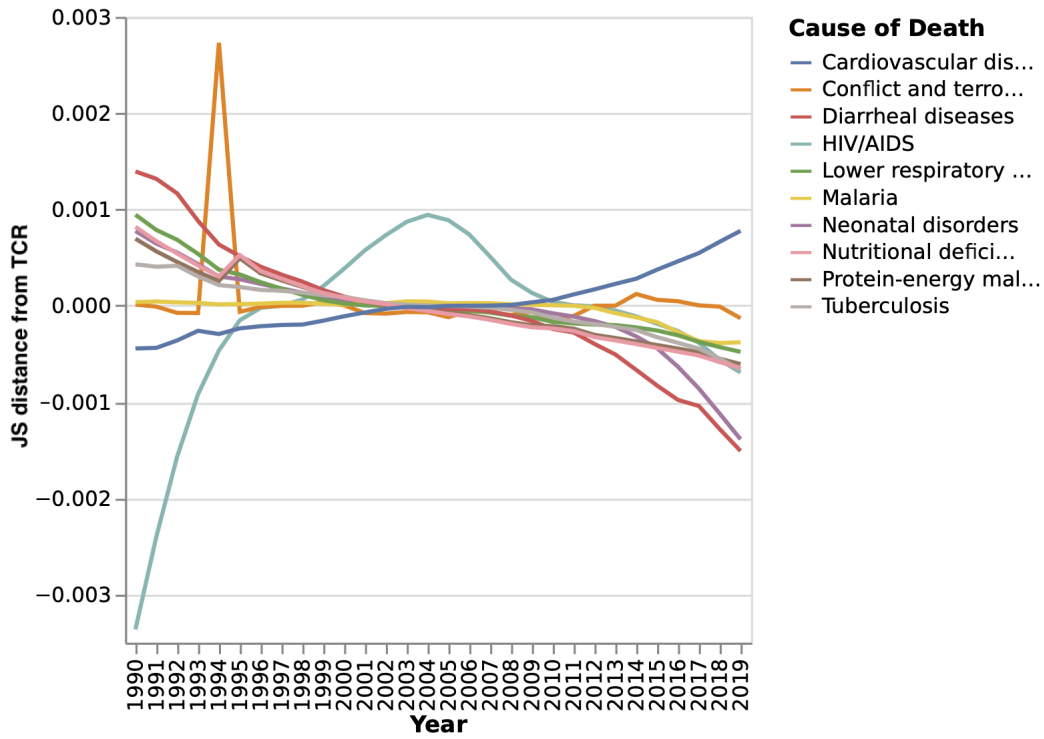


FIG. 2. Distance from the TCR of the 10 most highly variable (fluctuating along the timeline) causes of death in the CoD dataset. In 1994, for example, there is a spike in deaths from conflict, making it one of the primary reasons this year stands out significantly from the surrounding years, as seen in Figure 1.

exhibited the greatest fluctuations in their relative importance compared to their mean value in the *TCR*. For each time bin t , Equations 5 and 7 identify the Jensen-Shannon divergence of each element (feature) from their value in the *TCR*.

For each element $e \in \Omega$, we define its accumulated distance from the *TCR* as:

$$D_{js}(k) = \sum_{t \in N} |SP_t(k)| \quad (9)$$

Sorting D_{js} in descending order provides a ranking of feature variability:

$$D_{sp}^\downarrow = \text{sort}(D_{sp}, \text{descending}) \quad (10)$$

where D_{sp}^\downarrow represents the sorted version of D_{sp} , arranged in decreasing order:

$$D_{sp}^\downarrow(1) \geq D_{sp}^\downarrow(2) \geq \dots \geq D_{sp}^\downarrow(|\Omega|) \quad (11)$$

This ordering ensures that the most highly variable features along the timeline appear at the top.

Figure 2 presents the top 10 most highly variable causes of death over the 30-year period. Interestingly, while HIV was a major topic of public discussion during the 1990s, its peak in mortality occurred in 2004 and 2005. Additionally, notable is the growing number of deaths attributed to cardiovascular disease over the years, while deaths from diarrheal diseases show a steady decline during this period.

V. ANALYSIS OF TIMELINES OF TEXTUAL DATA: THE STATE OF THE UNION ADDRESSES 1790–2022 DATASET

Here, we use the State of the Union dataset¹²², consisting of the United States (US) State-of-the-Union (SOTU) addresses that were given by the various US presidents each year. The dataset we obtained contains 233 addresses delivered by 46 presidents, starting with President George Washington’s first SOTU address in 1790. The last address in our dataset is President Biden’s 2022 SOTU address. There were a few notable exceptional addresses within the dataset that we note here. SOTU addresses can be delivered either in writing or orally, and during the majority of the nineteenth century were delivered in writing. This changed in 1913, and since then, most addresses are given orally. In 1946, President Truman delivered a written address consisting of 25,000 words. In 1981, President Carter also delivered a written address. All addresses were included in our analysis. Generally speaking, SOTU’s have a defining place in the US and the world’s agenda. Presidents use these opportunities to communicate with the public, set forth their agenda, and make specific policy proposals while addressing the legislative institution¹²³. SOTU addresses have become a key tool in exercising presidential power and, as such, were the focus of much research, with respect to the topics raised in the addresses and their effect^{124,125}.

Working with the highly complex textual SOTU dataset, which contains well-known topics, events, and meaning, enables us to demonstrate LvS transformation process and the analytical power it provides in a meaningful yet easy-to-understand manner.

A. Preprocessing

To characterize the SOTU dataset using LvS, we consider each year as a time bin, dividing the period from 1790 to 2021 into 232 time bins. The address given each year is then represented as a term frequency distribution vector. Neglecting the order of the words or their grammar, a distribution vector represents the relative frequency of each term in the address. We further remove stop words such as "the", "a", "to" etc., and normalize by the length to create a probability distribution vector. As each year is a time bin, a president who served for four years and gave four addresses will have four probability frequency distribution vectors, one in each corresponding time bin. The resulted probability distributions across the timeline are of *various lengths*, containing different number of elements.

B. transformation

The first step is to create the *TCR*, as depicted in Eq. (2). The choice to calculate the mean across the time bins rather than to aggregate the frequency of each element all time bins and normalize it (as was the protocol in LPA²⁴) gives equal importance to each time bin. Thus, a time bin containing much information can not overshadow other time bins. In the case of SOTU, a very long address like Truman’s 1946 address would still only contribute 1/232 of the weight to the mean of each element.

The resulting SOTU *TCR* contains 20,136 terms. The ten most prevalent words across the years are *state, government, year, congress, united, nation, people, country, american, and may*. The least frequent word along the timeline is *buffer*.

We then create a time bin Surprisability Profile (SP) for each address, according to Eqs 5, 7, and 8. At each time bin in the SOTU dataset, the SP represents the terms that most distinguish that year’s presidential address, highlighting what is emphasized more and what is emphasized less, or missing, compared with the *TCR*.

C. Surprisability Profiles capturing presidential stylistic and topic choices

Here are a few examples of presidential style and topic choices, as found in the Surprisability Profile (SP). Notable for George Washington is his discussion of “provisions”, “appointments” of “commissions”, and “laws” and “institutions”. Yet, he seldom references the “world”, a highly prevalent term in addresses, ranked 14th in the *TCR*. Woodrow Wilson increased the use of

the terms “action” and “necessary” in 1916, referring to internal matters, while significantly reducing references to “peace”, “war”, or the “world”. This trend was reversed in 1917, a few months before the U.S. joined World War I. Similarly, in an abrupt change from Lyndon B. Johnson, Richard Nixon hardly mentions the “war” until 1974. Moving to more recent times, an interesting stylistic pattern in Barack Obama’s addresses is his frequent use of the word “know”, although its usage declines in each subsequent year, alongside a decreasing trend in references to the “government”. Another notable underused term is “condition”, a relatively common word. Obama rarely uses it, and when he does, he often refers to “pre-existing conditions”. Another interesting stylistic choice is Donald Trump’s lack of use of the word “may”, a highly prevalent term otherwise (ranked tenth in the *TCR*). Trump used the term twice in his first address in 2017 but did not use it at all in his subsequent speeches during that presidential term. Notable in his speeches is his frequent repetition of guest names.

To validate that the SPs capture important information about the presidents’ styles, we identify similarities between presidents based on their surprising terms in their addresses and cluster them accordingly. We then compare the resulting clustering to a well-established reference classification.

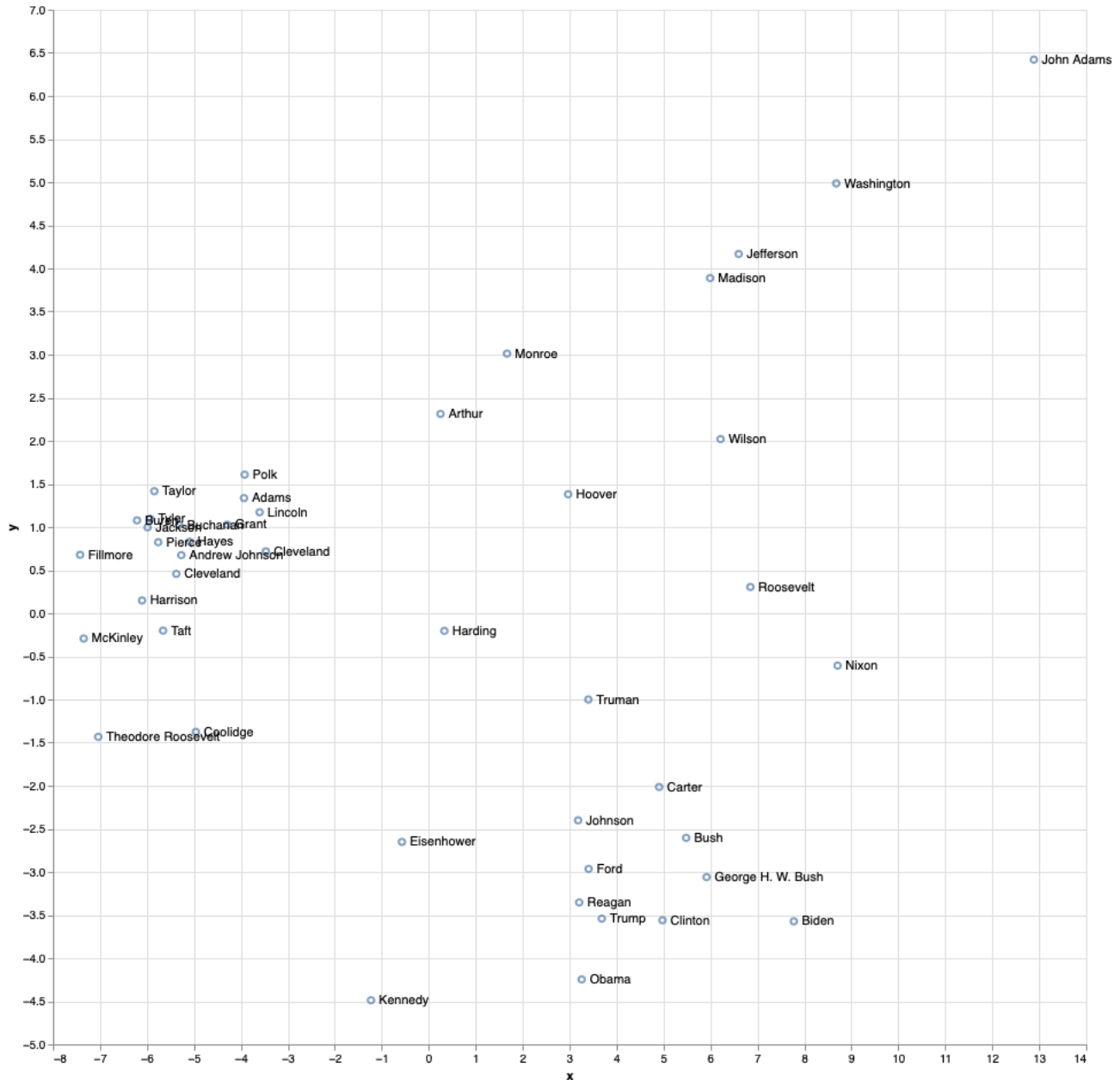


FIG. 3. Two-dimensional PCA representation of the differences across LvS’s transformation of presidential addresses. PCA1 (X-axis) accounts for 67% of the variance, while PCA2 (Y-axis) accounts for 6.8%.

Figure 3 presents a dimensionality reduction representation of a distance matrix computed for all presidents. To construct this matrix, each SOTU address given by a president was compared to all SOTU addresses given by other presidents using the Manhattan distance between their SPs. The average of these distances was then calculated for each presidential pair. Additionally, we computed intra-president distances to measure how consistent a president's SPs are across their own speeches. To validate our results, we reference the work of Jacques Savoy¹²⁶, who analyzed presidential speech similarities using text clustering. In a similar approach, Savoy applied PCA to a distance matrix computed between the presidents' speeches, focusing on part-of-speech usage. Their analysis contrasted the frequency of determiners and prepositions against pronouns, modal verbs, and adverbs. However, in their case, the two principal components accounted for 40.3% and 15.9% of the variance, while in our case, they account for 67% and 6.8%, respectively.

Our findings align with Savoy's in several aspects. Like us, they identify a distinct cluster on the left of Figure 3, including Presidents McKinley, Taft, Cleveland (twice), Hayes, Pierce, Harrison, Jackson, Theodore Roosevelt, Fillmore, and Coolidge. However, while we place President Hoover further from this group, Savoy positions him closer, though they also find no clear stylistic matches for his speeches.

Similarly, both analyses place Presidents Eisenhower, Kennedy, and Ford in the same region. However, our findings regarding Presidents Bush (both senior and junior), Reagan, Clinton, and Obama differ from Savoy's. That said, both studies find that Presidents Carter and Bush Sr. have relatively similar speech patterns. Notably, Savoy's analysis does not include Presidents Trump and Biden.

Overall, this comparison reinforces the validity of our method, demonstrating its ability to effectively capture stylistic patterns in presidential addresses.

D. Interpretable anomaly detection in SOTU Addresses over time

The figure provides a visual anomaly detection of SOTU addresses over the years, highlighting points where certain terms significantly deviate from the norm. By normalizing the values, the figure makes it easier to spot moments of linguistic or thematic change in presidential rhetoric.

Several notable patterns emerge in the data. A clear linguistic shift occurred when the U.S. entered World War I, but even earlier, in 1913, Woodrow Wilson introduced a significant change. The most surprising term of that year, *tonight*, reflects a major transition—before 1913, SOTU addresses were delivered in writing, whereas from that year onward, they were generally presented orally.

The 1942 SOTU address, delivered during World War II, contains the ten most surprising terms, which are color-coded: blue for overused terms and pink for underused ones. To maintain readability, the figure highlights the top 10 terms. The most overused surprising terms include *war*, *fighting*, *enemy*, *Hitler*, *victory*, *Japanese*, *production*, and *conquest*. Conversely, three commonly used words that are missing or significantly underused in Franklin D. Roosevelt's 1942 address are *law*, *public*, and *government*.

In 1951, six months after the Korean War began, Harry S. Truman delivered a speech marked by two key surprising terms: *free* and *Soviet*. These shifts in language reflect how presidential rhetoric adapts to major historical events, making them clear points of linguistic change.

1. Highly Variable SOTU Terms Across the Years

We present here the fluctuations of a few selected highly variable terms over time. These terms are among the most variable in SOTU addresses and were chosen because they exhibit distinct trends, highlighting different patterns of change in presidential rhetoric and thematic emphasis.

Figures 5, 6, and 7 illustrate how the usage of key terms—*government*, *America*, and *child*—has changed over time in SOTU addresses, capturing both their frequency and variability. Each figure consists of two panels: the upper panel represents the Jensen-Shannon distance from the *TCR*, highlighting how much the term's usage deviates from expected, while the lower panel shows its actual frequency across the years.

Examining Figure 5, which tracks the term *government*, we see that it was frequently mentioned throughout the 19th and early 20th centuries, peaking in importance at various points before declining significantly after 1980. The variability of this term also shows noticeable shifts, suggesting that while the word remained a key part of presidential rhetoric for a long time, its role in political discourse has changed, especially in modern addresses.

In Figure 6, the term *America* shows a gradual increase in both frequency and variability over time. Its presence in speeches was relatively low in the 19th century but saw a substantial rise from the mid-20th century onward, particularly during moments of national significance such as World War II, the Cold War, and post-9/11 addresses. This suggests a growing emphasis on national identity and unity in presidential rhetoric.

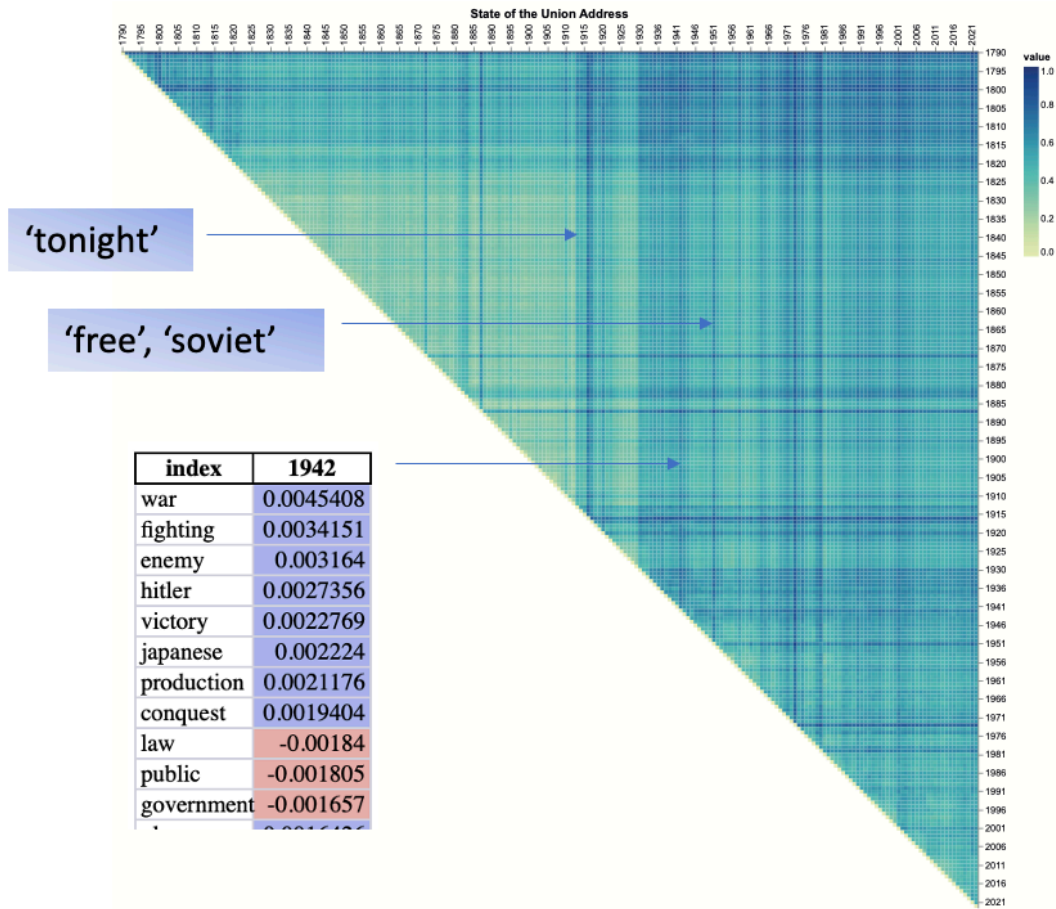


FIG. 4. Comparison of SPs found in SOTU addresses across all years. Values were normalized for readability. Annotations highlight notable points of change: the top surprising term in 1913; the ten most surprising terms in the 1942 SOTU address, with overused terms in blue and underused terms in pink; and the top two surprising terms in 1951.

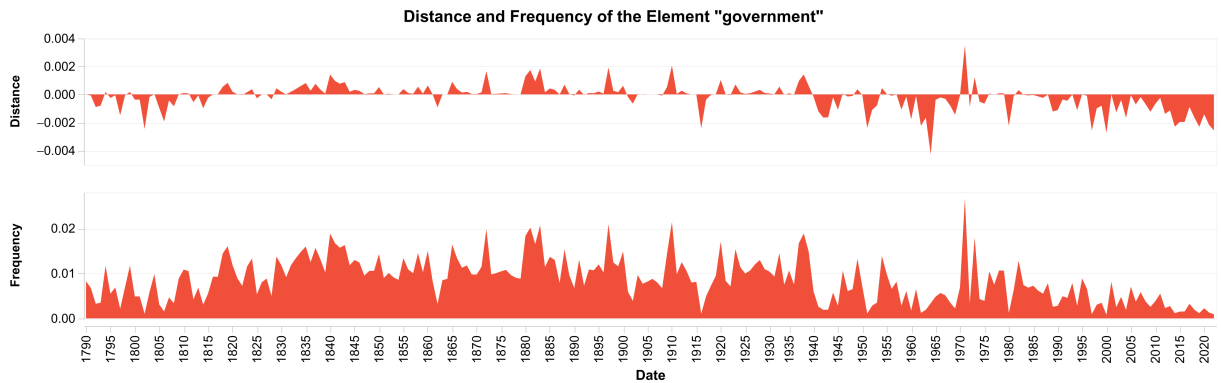


FIG. 5. Dynamics of the term *government*. The upper panel shows the variability by displaying the Jensen-Shannon distance from the *TCR*, while the lower panel shows the actual frequency along the timeline.

Similarly, Figure 7 shows that the term *child* was rarely mentioned before the 20th century, with noticeable peaks emerging in the 1960s and 1990s, suggesting that child welfare became a more prominent topic during this period, particularly peaking in President Clinton’s addresses. The increasing variability in later years indicates that while the term appears more frequently, its contextual significance may be evolving.

Overall, these figures highlight how LvS transformation can be used presidential rhetoric adapts to historical and political

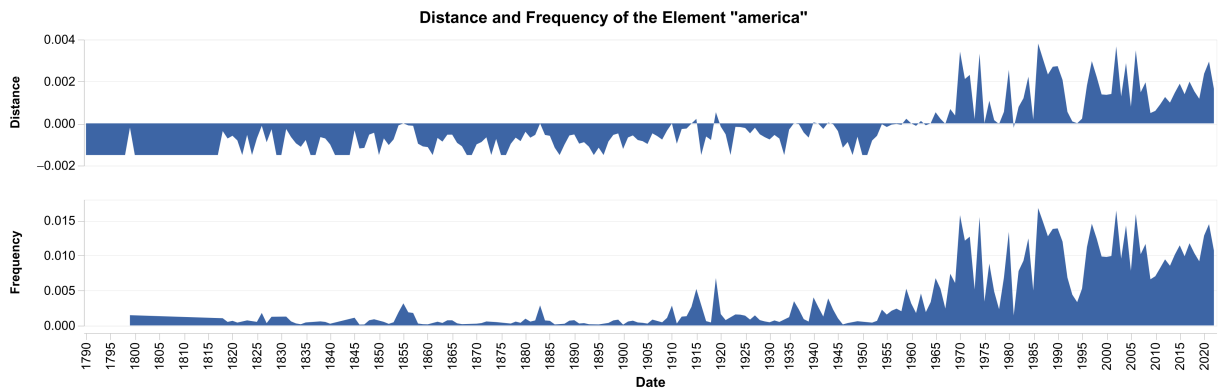


FIG. 6. Dynamics of the term *america*. The upper panel shows the variability by displaying the Jensen-Shannon distance from the *TCR*, while the lower panel shows the actual frequency along the timeline.

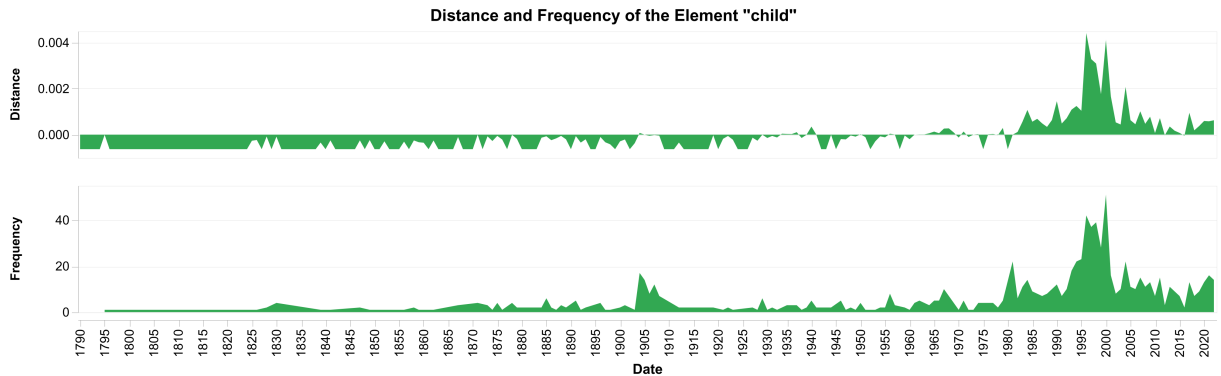


FIG. 7. Dynamics of the term *child*. The upper panel shows the variability by displaying the Jensen-Shannon distance from the *TCR*, while the lower panel shows the actual frequency along the timeline.

contexts, with some terms gaining prominence over time while others decline in usage. The variability patterns suggest that certain words, even when frequently used, can carry different connotations and importance depending on the era in which they appear.

VI. DISCUSSION AND CONCLUSION

Here, we introduced Learning via Surprisability (LvS) as a novel transformation approach, which is useful in characterizing high-dimensional time-series data through a representation of the timeline through Timeline Center Representation (*TCR*) and of the time bins through their Surprisability Profiles (SP). The SP of a time bin includes the most surprising elements in this time bin when the *TCR* is expected. LvS transformation provides a novel approach for analyzing high-dimensional timeline data, effectively addressing challenges such as high dimensionality, complex distributions, and sparsity. By drawing inspiration from cognitive science and the concept of surprisal, LvS identifies the most unexpected elements in a dataset, offering a powerful and interpretable method for anomaly detection and transformation. Unlike existing methods that either reduce dimensionality at the expense of interpretability or rely on predefined heuristics, LvS preserves context by emphasizing features that deviate the most from expected patterns.

The ability of LvS to detect anomalies and highlight significant deviations was demonstrated in multiple real-world datasets. In the SWaT dataset, where the goal was to detect cyber-physical anomalies in an industrial water treatment system, LvS performed on par with or better than state-of-the-art unsupervised anomaly detection methods such as Isolation Forest, Local Outlier Factor (LOF), and One-Class SVM. While conventional models struggled to find a balance between precision and recall, LvS consistently identified attack instances with high accuracy and recall. The approach of comparing each time bin to a timeline-wide expectation proved highly effective in flagging anomalies, which in this case corresponded to cyberattacks. The interpretability of LvS adds another layer of utility—rather than simply labeling an observation as an anomaly, it provides insight into the features responsible for the deviation. This is a key advantage over black-box machine learning models, which often

struggle to provide explanations for their decisions.

Beyond anomaly detection, LvS also excels at capturing contextual shifts over time. In the analysis of mortality causes worldwide, the transformation enabled a clear visualization of trends, outliers, and abrupt changes in global health data spanning three decades. While traditional statistical approaches focus on overall trends, LvS highlighted specific moments in time when major shifts occurred, such as the spike in deaths due to conflict in 1994, corresponding to the Rwandan genocide, or the unusual increase in mortality caused by natural disasters in 2004, 2008, and 2010. The ability to pinpoint such changes and, more importantly, to interpret the features responsible for them makes LvS a valuable tool for time-series analysis.

A similar effect was observed in the textual domain, where LvS was applied to the State of the Union addresses spanning more than two centuries. By transforming each speech into a surprisal-based representation, the method revealed stylistic shifts, policy priorities, and linguistic trends across different presidencies. For example, the sudden rise of war-related terms in 1917, before the U.S. entered World War I, and the dominance of military and conflict-related words in Roosevelt's 1942 address at the height of World War II were captured clearly through the transformation. At the same time, LvS identified less obvious patterns, such as the declining use of the word "government" over the last few decades or the unique stylistic tendencies of individual presidents. The clustering of presidents based on their surprisal profiles showed strong alignment with independent linguistic studies, reinforcing the validity of the transformation in capturing meaningful distinctions in writing style and thematic focus.

The LvS transformation stands in contrast with existing transformation and anomaly detection techniques, offering a distinctive approach that models changes over time rather than aggregating entity distributions into a single population-wide representation, as seen in Latent Personal Analysis (LPA)²⁴. Unlike LPA, which provides a structured representation of entities by capturing deviations from a global reference distribution, LvS dynamically constructs an evolving expectation of the timeline, enabling the detection of temporal shifts and anomalies. Similarly, while classical transformation methods such as PCA¹²⁷ and Fourier analysis¹⁶ offer effective dimensionality reduction, they often fail to preserve local interpretability, particularly in non-stationary datasets. Fourier transform and its variants are widely used for time-series analysis but are primarily designed for frequency decomposition rather than anomaly detection, limiting their ability to identify contextual outliers in high-dimensional datasets.

Beyond transformation methods, LvS also diverges from traditional and contemporary anomaly detection techniques. Classical statistical anomaly detection approaches, such as Gaussian mixture models³³, kernel density estimation¹²⁸, and Mahalanobis distance-based outlier detection⁶, rely on assumptions about the underlying data distribution, making them less effective in high-dimensional or sparse datasets where distributions are complex and non-Gaussian. More recent machine learning-based approaches, including deep autoencoders⁸⁰, generative adversarial networks (GANs) for anomaly detection¹²⁹, and one-class SVMs⁷⁹, offer state-of-the-art performance in identifying anomalies but often lack interpretability. These models typically function as black boxes, providing little insight into why a given observation is classified as anomalous. Moreover, methods such as Isolation Forest and LOF assess the degree of isolation of individual data points, but their effectiveness diminishes in high-dimensional spaces due to the curse of dimensionality⁹². Unlike these approaches, LvS retains both computational efficiency and interpretability by identifying the most surprising features that differentiate each time bin from the timeline's overall expectation, allowing users to understand and contextualize anomalies rather than treating them as abstract deviations.

Despite its advantages, LvS has several limitations that should be acknowledged. First, the method relies on the assumption that past distributions accurately represent expected behaviors, which may not always hold in rapidly evolving systems (also known as concept drift)^{130,131}. To address the challenge of concept drift, future work could integrate adaptive learning mechanisms that dynamically update the baseline distribution over time. One potential approach is to incorporate online learning models that continuously adjust the TCR in response to new data, ensuring that the method remains sensitive to evolving patterns^{132,133}. Second, LvS is inherently retrospective, making it unsuitable for real-time anomaly detection without further adaptations. Third, the selection of the surprisal threshold, which determines which features are included in a time bin's representation. While the current approach effectively captures anomalies across various datasets, it requires manual tuning of this threshold, which may not be optimal for all applications. An adaptive thresholding mechanism, possibly leveraging statistical significance tests or identifying the point of diminishing return when the contribution to the divergence is considered, could enhance the robustness of LvS in different domains.

Taken jointly, LvS provides a novel framework for transforming and analyzing high-dimensional timeline data, effectively bridging the gap between classical transformation techniques and modern anomaly detection methods. Its ability to highlight significant shifts while preserving contextual meaning makes it a promising tool for a wide range of applications, from cybersecurity monitoring and financial risk assessment to epidemiological studies and linguistic research.

Future directions include applications in more specialized fields, such as biomedical signal processing or fraud detection in financial transactions. Improvements that address its current limitations—such as adaptive thresholding, real-time processing, and domain-specific optimizations—could further expand its applicability and establish LvS as a standard approach for timeline analysis in complex datasets.

REFERENCES

- ¹F. Altıparmak, H. Ferhatosmanoglu, S. Erdal, and D. C. Trost, "Information mining over heterogeneous and high-dimensional time-series data in clinical trials databases," *IEEE Transactions on Information Technology in Biomedicine* **10**, 254–263 (2006).
- ²T. Ando and J. Bai, "Clustering huge number of financial time series: A panel data approach with high-dimensional predictors and factor structures," *Journal of the American Statistical Association* **112**, 1182–1198 (2017).
- ³R. Bodnar, T. Bodnar, and W. Schmid, "Sequential monitoring of high-dimensional time series," *Scandinavian Journal of Statistics* **50**, 962–992 (2023).
- ⁴V. Gadepally and J. Kepner, "Using a power law distribution to describe big data," in *2015 IEEE High Performance Extreme Computing Conference (HPEC)* (IEEE, 2015) pp. 1–5.
- ⁵P. Kanerva, "Hyperdimensional computing: An introduction to computing in distributed representation with high-dimensional random vectors," *Cognitive computation* **1**, 139–159 (2009).
- ⁶S. Thudumu, P. Branch, J. Jin, and J. Singh, "A comprehensive survey of anomaly detection techniques for high dimensional big data," *Journal of Big Data* **7**, 1–30 (2020).
- ⁷T. Miller, "Explanation in artificial intelligence: Insights from the social sciences," *Artificial intelligence* **267**, 1–38 (2019).
- ⁸D. Bertsimas and B. Van Parys, "Sparse high-dimensional regression," *The Annals of Statistics* **48**, 300–323 (2020).
- ⁹S. Manzhos and M. Ihara, "Advanced machine learning methods for learning from sparse data in high-dimensional spaces: A perspective on uses in the upstream of development of novel energy technologies," *Physchem* **2**, 72–95 (2022).
- ¹⁰D. Bertsimas and V. Digalakis Jr, "The backbone method for ultra-high dimensional sparse machine learning," *Machine Learning* **111**, 2161–2212 (2022).
- ¹¹N. H. Ibragimov, *Transformation groups applied to mathematical physics*, Vol. 3 (Springer Science & Business Media, 1984).
- ¹²N. Ahmed and K. R. Rao, *Orthogonal transforms for digital signal processing* (Springer Science & Business Media, 2012).
- ¹³J. Sahambi, S. Tandon, and R. Bhatt, "Using wavelet transforms for ecg characterization. an on-line digital signal processing system," *IEEE Engineering in Medicine and Biology Magazine* **16**, 77–83 (1997).
- ¹⁴R. A. Rossi, L. K. McDowell, D. W. Aha, and J. Neville, "Transforming graph data for statistical relational learning," *Journal of Artificial Intelligence Research* **45**, 363–441 (2012).
- ¹⁵M. A. Platas-Garza and J. A. de la O Serna, "Dynamic harmonic analysis through taylor–fourier transform," *IEEE Transactions on Instrumentation and Measurement* **60**, 804–813 (2010).
- ¹⁶R. N. Bracewell, "The fourier transform," *Scientific American* **260**, 86–95 (1989).
- ¹⁷W. Lu and F. Li, "Seismic spectral decomposition using deconvolutive short-time fourier transform spectrogram," *Geophysics* **78**, V43–V51 (2013).
- ¹⁸N. Beaudoin and S. S. Beauchemin, "An accurate discrete fourier transform for image processing," in *2002 International Conference on Pattern Recognition*, Vol. 3 (IEEE, 2002) pp. 935–939.
- ¹⁹B. D. Fulcher, "Feature-based time-series analysis," in *Feature engineering for machine learning and data analytics* (CRC press, 2018) pp. 87–116.
- ²⁰L. Lacasa, B. Luque, F. Ballesteros, J. Luque, and J. C. Nuno, "From time series to complex networks: The visibility graph," *Proceedings of the National Academy of Sciences* **105**, 4972–4975 (2008).
- ²¹Z.-K. Gao, M. Small, and J. Kurths, "Complex network analysis of time series," *Europhysics Letters* **116**, 50001 (2017).
- ²²G. Misitano, "Exploring the explainable aspects and performance of a learnable evolutionary multiobjective optimization method," *ACM Transactions on Evolutionary Learning and Optimization* **4**, 1–39 (2024).
- ²³T. Lazebnik, S. Bunimovich-Mendrazitsky, and A. Rosenfeld, "An algorithm to optimize explainability using feature ensembles," *Applied Intelligence* **54**, 2248–2260 (2024).
- ²⁴O. Mokryn and H. Ben-Shoshan, "Domain-based latent personal analysis and its use for impersonation detection in social media," *User Modeling and User-Adapted Interaction* **31**, 785–828 (2021).
- ²⁵U. Alon, O. Mokryn, and U. Hershberg, "Using domain based latent personal analysis of b cell clone diversity patterns to identify novel relationships between the b cell clone populations in different tissues," *Frontiers in immunology* **12**, 642673 (2021).
- ²⁶D. Jensen, M. Atighetchi, R. Vincent, and V. Lesser, "Learning quantitative knowledge for multiagent coordination TITLE2:," in *Proceedings of the 16th National Conference on Artificial Intelligence* (1999) pp. 24–31.
- ²⁷S. Kullback and R. A. Leibler, "On information and sufficiency," *The annals of mathematical statistics* **22**, 79–86 (1951).
- ²⁸R. Levy, "Memory and surprisal in human sentence comprehension," in *Sentence processing* (Psychology Press, 2013) pp. 90–126.
- ²⁹J. Hale, "A probabilistic earley parser as a psycholinguistic model," in *Second meeting of the north american chapter of the association for computational linguistics* (2001).
- ³⁰R. Levy, "Expectation-based syntactic comprehension," *Cognition* **106**, 1126–1177 (2008).
- ³¹D. Norris, "Putting it all together: a unified account of word recognition and reaction-time distributions," *Psychological review* **116**, 207 (2009).
- ³²J. Hale, "Information-theoretical complexity metrics," *Language and Linguistics Compass* **10**, 397–412 (2016).
- ³³L. Li, R. J. Hansman, R. Palacios, and R. Welsch, "Anomaly detection via a gaussian mixture model for flight operation and safety monitoring," *Transportation Research Part C: Emerging Technologies* **64**, 45–57 (2016).
- ³⁴P. Bholowalia and A. Kumar, "Ebk-means: A clustering technique based on elbow method and k-means in wsn," *International Journal of Computer Applications* **105** (2014).
- ³⁵K. R. Rao and P. C. Yip, *The transform and data compression handbook* (CRC press, 2018).
- ³⁶R. M. Lewitt, "Reconstruction algorithms: transform methods," *Proceedings of the IEEE* **71**, 390–408 (1983).
- ³⁷J. Duchene and S. Leclercq, "An optimal transformation for discriminant and principal component analysis," *IEEE Transactions on Pattern Analysis and Machine Intelligence* **10**, 978–983 (1988).
- ³⁸T. Lazebnik and L. Simon-Keren, "Knowledge-integrated autoencoder model," *Expert Systems with Applications* **252**, 124108 (2024).
- ³⁹F. Ayaz, "Solutions of the system of differential equations by differential transform method," *Applied Mathematics and Computation* **147**, 547–567 (2004).
- ⁴⁰Y. Keskin and G. Oturanc, "Reduced differential transform method for partial differential equations," *International Journal of Nonlinear Sciences and Numerical Simulation* **10**, 741–750 (2009).
- ⁴¹Z. Odibat, S. Momani, and V. S. Erturk, "Generalized differential transform method: application to differential equations of fractional order," *Applied Mathematics and Computation* **197**, 467–477 (2008).
- ⁴²D. Alsdorf, "Noise reduction in seismic data using fourier correction coefficient filtering," *Geophysics* **62**, 1617–1627 (1997).
- ⁴³H. Bahouri, *Fourier analysis and nonlinear partial differential equations* (Springer, 2011).
- ⁴⁴V. Serov et al., *Fourier series, Fourier transform and their applications to mathematical physics*, Vol. 197 (Springer, 2017).
- ⁴⁵J. L. Schiff, *The Laplace transform: theory and applications* (Springer Science & Business Media, 1999).

- ⁴⁶M. Farge *et al.*, “Wavelet transforms and their applications to turbulence,” *Annual review of fluid mechanics* **24**, 395–458 (1992).
- ⁴⁷H. Wilber, A. Damle, and A. Townsend, “Data-driven algorithms for signal processing with trigonometric rational functions,” *SIAM journal on scientific computing* **44**, C185–C209 (2022).
- ⁴⁸J. N. Kutz, *Data-driven modeling & scientific computation: methods for complex systems & big data* (OUP Oxford, 2013).
- ⁴⁹P. Jain, B. Kulis, J. V. Davis, and I. S. Dhillon, “Metric and kernel learning using a linear transformation,” *The Journal of Machine Learning Research* **13**, 519–547 (2012).
- ⁵⁰V. R. Boppana, “Machine learning and ai learning: Understanding the revolution,” *Journal of Innovative Technologies* **5** (2022).
- ⁵¹K. Gurney, *An introduction to neural networks* (CRC press, 2018).
- ⁵²G. Zhong, L.-N. Wang, X. Ling, and J. Dong, “An overview on data representation learning: From traditional feature learning to recent deep learning,” *The Journal of Finance and Data Science* **2**, 265–278 (2016).
- ⁵³W. H. L. Pinaya, S. Vieira, R. Garcia-Dias, and A. Mechelli, “Autoencoders,” in *Machine learning* (Elsevier, 2020) pp. 193–208.
- ⁵⁴D. P. Kingma and M. Welling, “An introduction to variational autoencoders,” *Foundations and Trends® in Machine Learning* **12**, 307–392 (2019).
- ⁵⁵J. Rocha, C. M. Viana, and S. Oliveira, *Time Series Analysis* (IntechOpen, Rijeka, 2024).
- ⁵⁶J. Zhang, J. Zhou, M. Tang, H. Guo, M. Small, and Y. Zou, “Constructing ordinal partition transition networks from multivariate time series,” *Scientific reports* **7**, 7795 (2017).
- ⁵⁷M. Small, M. McCullough, and K. Sakellariou, “Ordinal network measures—quantifying determinism in data,” in *2018 IEEE International Symposium on Circuits and Systems (ISCAS)* (IEEE, 2018) pp. 1–5.
- ⁵⁸H. Miller and O. Mokryn, “Constant state of change: engagement inequality in temporal dynamic networks,” *Applied Network Science* **4**, 1–14 (2019).
- ⁵⁹H. Miller and O. Mokryn, “Size agnostic change point detection framework for evolving networks,” *Plos one* **15**, e0231035 (2020).
- ⁶⁰Y. Marmor, A. Abbey, Y. Shahar, and O. Mokryn, “Assessing individual risk and the latent transmission of covid-19 in a population with an interaction-driven temporal model,” *Scientific Reports* **13**, 12955 (2023).
- ⁶¹O. Mokryn, A. Abbey, Y. Marmor, and Y. Shahar, “Evaluating the dynamic interplay of social distancing policies regarding airborne pathogens through a temporal interaction-driven model that uses real-world and synthetic data,” *Journal of Biomedical Informatics* **151**, 104601 (2024).
- ⁶²A. Abbey, Y. Shahar, and O. Mokryn, “Analysis of the competition among viral strains using a temporal interaction-driven contagion model,” *Scientific Reports* **12**, 9616 (2022).
- ⁶³V. Chandola, A. Banerjee, and V. Kumar, “Anomaly detection: A survey,” *ACM computing surveys (CSUR)* **41**, 1–58 (2009).
- ⁶⁴G. Pang, c. Shen, L. Cao, and A. Van Den Hengel, “Deep learning for anomaly detection: A review,” *ACM Computing Surveys (CSUR)* **54**, 1–38 (2021).
- ⁶⁵X. Xu, H. Liu, and M. Yao, “Recent progress of anomaly detection,” *Complexity* **2019**, 2686378 (2019).
- ⁶⁶M. Ahmed, A. N. Mahmood, and R. Islam, “A survey of anomaly detection techniques in financial domain,” *Future Generation Computer Systems* **55**, 278–288 (2016).
- ⁶⁷C. W. Ten, J. Hong, and C. C. Liu, “Anomaly detection for cybersecurity of the substations,” *IEEE Transactions on Smart Grid* **2**, 865–873 (2011).
- ⁶⁸N. R. Prasad, S. Almanza-García, and T. T. Lu, “Anomaly detection,” *Computers, Materials, & Continua* **14**, 1–22 (2010).
- ⁶⁹R. A. A. Habeeb, F. Nasaruddin, A. Gani, I. A. T. Hashem, E. Ahmed, and M. Imran, “Real-time big data processing for anomaly detection: A survey,” *International Journal of Information Management* **45**, 289–307 (2019).
- ⁷⁰W. Jia, R. M. Shukla, and S. Sengupta, “Anomaly detection using supervised learning and multiple statistical methods,” in *2019 18th IEEE International Conference on Machine Learning and Applications (ICMLA)* (IEEE, 2019) pp. 1291–1297.
- ⁷¹N. Görmitz, M. Kloft, K. Rieck, and U. Brefeld, “Toward supervised anomaly detection,” *Journal of Artificial Intelligence Research* **46**, 235–262 (2013).
- ⁷²A. B. Nassif, M. A. Talib, Q. Nasir, and F. M. Dakalbab, “Machine learning for anomaly detection: A systematic review,” *IEEE Access* **9**, 78658–78700 (2021).
- ⁷³J. P. Barnard and C. Aldrich, “Detecting outliers in multivariate process data by using convex hulls,” in *Computer Aided Chemical Engineering*, Vol. 8 (Elsevier, 2000) pp. 103–107.
- ⁷⁴K. Cohen and Q. Zhao, “Active hypothesis testing for anomaly detection,” *IEEE Transactions on Information Theory* **61**, 1432–1450 (2015).
- ⁷⁵G. B. P. Costa, M. Ponti, and A. C. Frery, “Partially supervised anomaly detection using convex hulls on a 2d parameter space,” in *Partially Supervised Learning: Second IAPR International Workshop, PSL 2013, Nanjing, China, May 13-14, 2013, Revised Selected Papers 2* (Springer, 2013) pp. 1–8.
- ⁷⁶E. Alpaydin, *Introduction to Machine Learning* (MIT Press, 2020).
- ⁷⁷D. Wang and Y. Shang, “A new active labeling method for deep learning,” in *2014 International Joint Conference on Neural Networks (IJCNN)* (IEEE, 2014) pp. 112–119.
- ⁷⁸L. M. Manevitz and M. Yousef, “One-class svms for document classification,” *Journal of machine Learning research* **2**, 139–154 (2001).
- ⁷⁹P. Oza and V. M. Patel, “One-class convolutional neural network,” *IEEE Signal Processing Letters* **26**, 277–281 (2018).
- ⁸⁰C. Zhou and R. C. Paffenroth, “Anomaly detection with robust deep autoencoders,” in *Proceedings of the 23rd ACM SIGKDD international conference on knowledge discovery and data mining* (2017) pp. 665–674.
- ⁸¹Z. Cheng, C. Zou, and J. Dong, “Outlier detection using isolation forest and local outlier factor,” in *Proceedings of the conference on research in adaptive and convergent systems* (2019) pp. 161–168.
- ⁸²A. Boukerche, L. Zheng, and O. Alfandi, “Outlier detection: Methods, models, and classification,” *ACM Computing Surveys (CSUR)* **53**, 1–37 (2020).
- ⁸³P. Novello, Y. Prudent, J. Dalmau, C. Friedrich, and Y. Pequignot, “Improving out-of-distribution detection by combining existing post-hoc methods,” *arXiv preprint arXiv:2407.07135* (2024).
- ⁸⁴M. E. Newman, “Power laws, pareto distributions and zipf’s law,” *Contemporary physics* **46**, 323–351 (2005).
- ⁸⁵J. Sun, H. Zhang, Q. Zhang, and H. Chen, “Balancing exploration and exploitation in multiobjective evolutionary optimization,” in *Proceedings of the Genetic and Evolutionary Computation Conference Companion* (2018) pp. 199–200.
- ⁸⁶J. Chen, B. Xin, Z. Peng, L. Dou, and J. Zhang, “Optimal contraction theorem for exploration–exploitation tradeoff in search and optimization,” *IEEE Transactions on Systems, Man, and Cybernetics-Part A: Systems and Humans* **39**, 680–691 (2009).
- ⁸⁷K. Sun, “Explanation of log-normal distributions and power-law distributions in biology and social science,” *Department of Physics, University of Illinois at Urbana-Champaign*, Tech. Rep (2004).
- ⁸⁸T. Lazebnik, Y. Golov, R. Gurka, A. Harari, and A. Liberzon, “Exploration–exploitation model of moth-inspired olfactory navigation,” *Journal of the Royal Society Interface* **21**, 20230746 (2024).
- ⁸⁹G. Lombardo, M. Tomaiuolo, M. Mordonini, G. Codeluppi, and A. Poggi, “Mobility in unsupervised word embeddings for knowledge extraction—the scholars’ trajectories across research topics,” *Future Internet* **14**, 25 (2022).
- ⁹⁰V. Ntranos, G. M. Kamath, J. M. Zhang, L. Pachter, and D. N. Tse, “Fast and accurate single-cell rna-seq analysis by clustering of transcript-compatibility counts,” *Genome biology* **17**, 112 (2016).
- ⁹¹G. Zipf, “Human behavior and the principle of least effort.” Addison Wesley, Cambridge, Massachusetts (1949).

- ⁹²M. Verleysen and D. François, “The curse of dimensionality in data mining and time series prediction,” in *International work-conference on artificial neural networks* (Springer, 2005) pp. 758–770.
- ⁹³C. C. Aggarwal, A. Hinneburg, and D. A. Keim, “On the surprising behavior of distance metrics in high dimensional space,” in *Database theory—ICDT 2001: 8th international conference London, UK, January 4–6, 2001 proceedings 8* (Springer, 2001) pp. 420–434.
- ⁹⁴U. Muaz and S. Sobolevsky, “Transfer learning from an auxiliary discriminative task for unsupervised anomaly detection,” arxiv (2019), 10.48550/arxiv.1912.02864.
- ⁹⁵D. Wei, J. Zheng, and H. Qu, “Anomaly detection for blueberry data using sparse autoencoder-support vector machine,” *PeerJ Computer Science* **9**, e1214 (2023).
- ⁹⁶S. Suboh, I. A. Aziz, S. M. Shaharudin, S. A. Ismail, and H. Mahdin, “A systematic review of anomaly detection within high dimensional and multivariate data,” *JOIV : International Journal on Informatics Visualization* **7**, 122 (2023).
- ⁹⁷S. Prandl, M. Lazarescu, D. S. Pham, S. T. Soh, and S. Kak, “An investigation of power law probability distributions for network anomaly detection,” in *2017 IEEE Security and Privacy Workshops (SPW)* (IEEE, 2017) pp. 217–222.
- ⁹⁸T. Lazebnik and D. Gorlitsky, “Can we mathematically spot the possible manipulation of results in research manuscripts using benford’s law?” *Data* **8**, 165 (2023).
- ⁹⁹Z. Ghahramani, “Unsupervised learning,” in *Summer school on machine learning* (Springer, 2003) pp. 72–112.
- ¹⁰⁰U. Itai, A. Bar Ilan, and T. Lazebnik, “Tighten the lasso: A convex hull volume-based anomaly detection method,” arXiv (2025).
- ¹⁰¹X. Zhang, P. Wei, and Q. Wang, “A hybrid anomaly detection method for high dimensional data,” *PeerJ Computer Science* **9**, e1199 (2023).
- ¹⁰²H. Song, Z. Jiang, A. Men, and B. Yang, “A hybrid semi-supervised anomaly detection model for high-dimensional data,” *Computational Intelligence and Neuroscience* **2017**, 1–9 (2017).
- ¹⁰³L. Zhang, J. Lin, and R. Karim, “An angle-based subspace anomaly detection approach to high-dimensional data: with an application to industrial fault detection,” *Reliability Engineering & System Safety* **142**, 482–497 (2015).
- ¹⁰⁴A. Deng and B. Hooi, “Graph neural network-based anomaly detection in multivariate time series,” *Proceedings of the AAAI Conference on Artificial Intelligence* **35**, 4027–4035 (2021).
- ¹⁰⁵D. Li, D. Chen, B. Jin, L. Shi, J. Goh, and S. Ng, “Mad-gan: multivariate anomaly detection for time series data with generative adversarial networks,” *Lecture Notes in Computer Science*, 703–716 (2019).
- ¹⁰⁶M. Mozaffari, K. Doshi, and Y. Yilmaz, “Online multivariate anomaly detection and localization for high-dimensional settings,” *Sensors* **22**, 8264 (2022).
- ¹⁰⁷H. J. Shin, D.-H. Eom, and S.-S. Kim, “One-class support vector machines—an application in machine fault detection and classification,” *Computers & Industrial Engineering* **48**, 395–408 (2005).
- ¹⁰⁸O. Alghushairy, R. Alsin, T. Soule, and X. Ma, “A review of local outlier factor algorithms for outlier detection in big data streams,” *Big Data and Cognitive Computing* **5**, 1 (2020).
- ¹⁰⁹T. Chari and L. Pachter, “The specious art of single-cell genomics,” *PLOS Computational Biology* **19**, e1011288 (2023).
- ¹¹⁰R. Foorthuis, “On the nature and types of anomalies: a review of deviations in data,” *International journal of data science and analytics* **12**, 297–331 (2021).
- ¹¹¹S. DeDeo, R. X. Hawkins, S. Klingenstein, and T. Hitchcock, “Bootstrap methods for the empirical study of decision-making and information flows in social systems,” *Entropy* **15**, 2246–2276 (2013).
- ¹¹²O. Lombardi, F. Holik, and L. Vanni, “What is shannon information?” *Synthese* **193**, 1983–2012 (2016).
- ¹¹³C. W. Granger, “Extracting information from mega-panels and high-frequency data,” *Statistica Neerlandica* **52**, 258–272 (1998).
- ¹¹⁴B. Bigi, “Using kullback-leibler distance for text categorization,” in *Advances in Information Retrieval: 25th European Conference on IR Research, ECIR 2003, Pisa, Italy, April 14–16, 2003. Proceedings* (Springer, 2003) pp. 305–319.
- ¹¹⁵In later works, we intend to expand to a streaming setting.
- ¹¹⁶L. Yuan and K. J. Forshay, “Using swat to evaluate streamflow and lake sediment loading in the xinjiang river basin with limited data,” *Water* **12**, 39:1–20 (2019).
- ¹¹⁷M. Bozdal, K. Ileri, and A. Ozkahraman, “Comparative analysis of dimensionality reduction techniques for cybersecurity in the swat dataset,” *The Journal of Supercomputing* **80**, 1059–1079 (2024).
- ¹¹⁸M. Bozdal, “Security through digital twin-based intrusion detection: A swat dataset analysis,” in *2023 16th International Conference on Information Security and Cryptology (ISCTurkiye)* (IEEE, 2023) pp. 1–6.
- ¹¹⁹J. Goh, S. Adepu, K. N. Junejo, and A. Mathur, “A dataset to support research in the design of secure water treatment systems,” in *Critical Information Infrastructures Security: 11th International Conference, CRITIS 2016, Paris, France, October 10–12, 2016, Revised Selected Papers 11* (Springer, 2017) pp. 88–99.
- ¹²⁰C. J. Murray, “The global burden of disease study at 30 years,” *Nature medicine* **28**, 2019–2026 (2022).
- ¹²¹H. Ritchie, F. Spooner, and M. Roser, “Causes of death,” *Our World in Data* (2018), <https://ourworldindata.org/causes-of-death>.
- ¹²²J. Woolley and G. Peters, “The american presidency project,” (2022).
- ¹²³D. R. Hoffman and A. D. Howard, *Addressing the State of the Union: The Evolution And Impact of the Presidents’s Big Speech* (Lynne Rienner Publishers, 2006).
- ¹²⁴J. A. Linder, J. Ma, D. W. Bates, B. Middleton, and R. S. Stafford, “Electronic health record use and the quality of ambulatory care in the united states,” *Archives of internal medicine* **167**, 1400–1405 (2007).
- ¹²⁵J. L. Tobin, C. J. Schneider, and D. Leblang, “Framing unpopular foreign policies,” *American Journal of Political Science* **66**, 947–960 (2022).
- ¹²⁶J. Savoy, “Text clustering: An application with the state of the union addresses,” *Journal of the Association for Information Science and Technology* **66**, 1645–1654 (2015).
- ¹²⁷K. P. F.R.S., “Liiv. on lines and planes of closest fit to systems of points in space,” *The London, Edinburgh, and Dublin Philosophical Magazine and Journal of Science* **2**, 559–572 (1901).
- ¹²⁸B. W. Silverman, *Density estimation for statistics and data analysis* (Routledge, 2018).
- ¹²⁹H. Zenati, C. S. Foo, B. Lecouat, G. Manek, and V. R. Chandrasekhar, “Efficient gan-based anomaly detection,” arXiv preprint arXiv:1802.06222 (2018).
- ¹³⁰T. Lazebnik, H. Weitman, Y. Goldberg, and G. A. Kaminka, “Rivendell: Project-based academic search engine,” arXiv (2022).
- ¹³¹J. Lu, A. Liu, F. Dong, F. Gu, J. Gama, and G. Zhang, “Learning under concept drift: A review,” *IEEE transactions on knowledge and data engineering* **31**, 2346–2363 (2018).
- ¹³²T. Lazebnik, “Pulling the carpet below the learner’s feet: Genetic algorithm to learn ensemble machine learning model during concept drift,” arXiv (2024).
- ¹³³H. Guo, H. Li, N. Sun, Q. Ren, A. Zhang, and W. Wang, “Concept drift detection and accelerated convergence of online learning,” *Knowledge and Information Systems* **65**, 1005–1043 (2023).